

The non-linear correlation function and the shapes of virialized halos

Ravi K. Sheth¹ and Bhuvnesh Jain²

¹ *Berkeley Astronomy Department, University of California, Berkeley, CA 94720*

² *Max-Planck-Institut für Astrophysik, Karl-Schwarzschild-Strasse 1, 85748 Garching, Germany*

Email: sheth@astron.berkeley.edu, bjain@mpa-garching.mpg.de

9 October 2018

ABSTRACT

The correlation function $\xi(r)$ of matter in the non-linear regime is assumed to be determined by the density profiles $\rho(r)$ and the mass distribution $n(M)$ of virialized halos. The Press–Schechter approach is used to compute $n(M)$, and the stable clustering hypothesis is used to determine the density profiles of these Press–Schechter halos. Thus, the shape and amplitude of $\xi(r)$ on small scales is related to the initial power spectrum of density fluctuations.

The case of clustering from scale-free initial conditions is treated in detail. If n is the slope of the initial power spectrum of density fluctuations, then stable clustering requires that $\xi(r) \propto r^{-\gamma}$, where γ is a known function of n . If halo–halo correlations can be neglected, then $\rho(r) \propto r^{-\epsilon}$, where $\epsilon = (\gamma + 3)/2 = 3(4 + n)/(5 + n)$. For all values of n of current interest, this slope is steeper than the value $3(3 + n)/(4 + n)$ that was obtained by Hoffman & Shaham in their treatment of the shapes of the outer regions of collapsed halos. Our main result is a prediction for the amplitude of the non-linear correlation function. The predicted amplitude and its dependence on n are in good quantitative agreement with N -body simulations of self-similar clustering.

If stable clustering is a good approximation only inside the half-mass radii of Press–Schechter halos, then the density contrast required for the onset of stable clustering can be estimated. This density contrast is in the range $\sim 300 - 600$ and increases with the initial slope n , in agreement with estimates from N -body simulations.

Key words: cosmology: theory – dark matter.

1 INTRODUCTION

Large-scale structure in the universe is thought to arise through the gravitational clustering of matter. In the non-linear regime most of the dark matter is in bound halos which have separated out from the expanding background. Therefore the auto-correlation function, $\xi(r)$, of the dark matter is closely related to the shapes of halos. In this paper we explore the consequences of this connection for the shape and amplitude of $\xi(r)$ on small scales.

There are two approximations that are commonly used to describe the evolution of gravitational clustering in the non-linear regime. The first is the assumption that, in this regime, the clustering is statistically stable. By this, one usually means that non-linear, virialized objects no longer participate in the expansion of the background Universe; they maintain their shapes in physical coordinates, so they shrink in comoving coordinates (e.g. Peebles 1965, 1980). The second approximation was first formulated by Press &

Schechter (1974). They assumed that, on average, structures collapse spherically and then virialize, with initially more dense regions collapsing first, and less dense regions collapsing later. Further, they assumed that when they virialize, all halos have the same density (about 200 times the background density at the time of virialization) whatever their mass. By applying these assumptions to an initially Gaussian density field, they derived the distribution of halos as a function of mass. In the Press–Schechter approach, the clustering is hierarchical, and virialized halos at a given epoch are progenitors of the halos that virialize at a later epoch. It is not obvious that these two idealizations, stable clustering, and virialization at a fixed multiple of the background density at the time of virialization, are compatible.

For example, consider a Press–Schechter halo with uniform density (it has a ‘tophat’ density profile). Assume that at the time it virializes, say t_1 , it has mass M_1 and density $178\rho_b(t_1)$. This sets its radius R_1 . In the Press–Schechter approach, at some later time $t_2 > t_1$, it will

have merged with other halos into an object of greater mass $M_2 > M_1$. This more massive object will have density $178 \rho_b(t_2) < 178 \rho_b(t_1)$. On the other hand, if stable clustering is correct, then the core M_1 within R_1 will still have density $178 \rho_b(t_1)$ so that the shell of mass $(M_2 - M_1)$ around the core must be less dense than the core itself. Thus, if it had a tophat density profile at time t_1 , then the halo will not have a tophat density profile at the epoch t_2 . In other words, if Press–Schechter halos are to evolve consistently with the stable clustering assumption, then they cannot have tophat density profiles. This toy example illustrates that by requiring consistency between Press–Schechter and the stability approximation we can constrain the allowed density profiles of halos.

In particular, it is known that the stable clustering approximation allows one to constrain the shape of $\xi(r)$ in the non-linear regime (e.g., Peebles 1974a; section 26 in Peebles 1980; section 5.4 in Padmanabhan 1993). Section 2 uses this stable clustering shape of $\xi(r)$ to constrain the density profiles of Press–Schechter halos. The formalism of McClelland and Silk (1977) is then used to compute the amplitude of $\xi(r)$ in the nonlinear regime. The predicted amplitude is compared with the results of N-body simulations. The density profile inferred in Section 2 is different from the value that is obtained in other descriptions of spherical collapse, such as the Hoffman-Shaham model. Section 3 discusses the reasons for the difference. Section 4 studies the density contrast required for the onset of stable clustering. It argues that only the cores of Press–Schechter halos are likely to have evolved consistently with both Press–Schechter and stable clustering. This has the consequence that the density required for the onset of stable clustering should be an increasing function of n , where n is the slope of the power spectrum of initial fluctuations. Section 5 discusses the case of non-power law density profiles and summarizes the results.

2 THE CORRELATION FUNCTION IN THE NON-LINEAR REGIME

In the highly non-linear regime, stable clustering may be a good approximation. This section combines the stable clustering hypothesis with the Press–Schechter model to compute the shape and amplitude of the correlation function $\xi(r)$. We consider first some simple and general properties of ξ .

2.1 Stable clustering and the density profile

Consider the auto-correlation function of matter $\xi(r)$ within a single halo. If the density profile of the halo is a power law,

$$\rho(r) = Ar^{-\epsilon}, \quad (1)$$

then $\xi(r)$ is

$$\xi(r) \propto \int d^3s \rho(\vec{s}) \rho(\vec{r} + \vec{s}) \propto \int ds s^2 s^{-\epsilon} |\vec{r} + \vec{s}|^{-\epsilon} \quad (2)$$

which is just a convolution of the density profile with itself. When the initial profile satisfies $3/2 < \epsilon < 3$, then the integral converges to give a power law form for the correlation function (Peebles 1974b; McClelland & Silk 1977):

$$\xi(r) \propto r^{-\gamma}, \quad \text{where } \gamma = 2\epsilon - 3. \quad (3)$$

If the density profile is a power law with slope ϵ on small scales, but has a cutoff on large scales, then the correlation function is also a power law, with slope γ given by equation (3) on small scales, but with a cutoff on larger scales.

Assuming that all matter is in halos of various masses, $\xi(r)$ depends on correlations within halos (essentially the density profile), correlations between halos, and the distribution of halo masses and radii. McClelland & Silk (1977) show that if all halos have the same mass and radius, and these halos are randomly placed in space (so that there are no halo–halo correlations), then the above result (equation 3) still relates the shape of ξ to the density profile ρ . They also show that, for randomly placed halos having a range of different masses, but the same density profile, an integral over mass must be included. This integral affects the amplitude, but not the shape of ξ . (If the density profile has a mass dependent cutoff, then the position of the ‘knee’ in ξ will depend on the number density of halos as a function of halo mass.)

Of course, if the halos are not randomly distributed, then their correlations will change the shape of ξ . Since halos are likely to be correlated with each other, the relation (equation 3) between the shapes of ξ and ρ would seem to be of limited applicability. However, if we restrict attention to small scales (the highly non-linear regime), then, for sufficiently small separations r , both members of each pair of particles will almost certainly be drawn from the same halo. This means that, for small separations, the shape of the correlation function is not affected by halo–halo correlations. If the halo–halo correlation function can be neglected, then we can use the formalism of McClelland & Silk (1977) to compute the shape and amplitude of $\xi(r)$ in the non-linear regime. To do so, however, we must know the density profiles of halos, and the number density of halos as a function of halo mass.

In the highly non-linear regime, stable clustering is a good approximation, and it can be used to constrain the shapes of virialized halos. For clustering from scale-free initial conditions, Davis & Peebles (1977) show that the BBGKY hierarchy of equations admit self-similar solutions (Peebles 1980; Section 73). They show that, in the stable clustering regime, $\xi(r)$ must be a power law: $\xi(r) \propto r^{-\gamma}$ with $\gamma = 3(3+n)/(5+n)$, where n is the slope of the initial spectrum $P(k) \propto k^n$. This form for $\xi(r)$, combined with equation (3), yields a value for ϵ in the stable clustering regime:

$$\epsilon_{\text{sc}} = \frac{\gamma + 3}{2} = \frac{3(4+n)}{(5+n)}, \quad \text{for } n > -3. \quad (4)$$

Note that whereas ϵ_{sc} may be thought of as the slope of the two-point correlation function, subject to the constraint that one member of each pair of particles is certainly at the center of a halo, γ is the slope of the correlation function when the locations of the members of each pair are unconstrained. For $0 < \gamma < 3$, equation (4) shows that $\epsilon > \gamma$, which means that the correlation function centered on peaks is steeper than the unconstrained correlation function. This behaviour is similar to that of peaks associated with Gaussian random fields; the density profile of a typical spherically averaged Gaussian peak is steeper than the unconstrained

correlation function of the Gaussian field (Bardeen et al. 1986).

In the remainder of this paper we will use this density profile $\rho(r) \propto r^{-\epsilon_{\text{sc}}}$ to describe the shapes of virialized halos. The differences between this profile and that suggested by Hoffman & Shaham (1985) are discussed in Section 3. The effects of non-power law density profiles such as that proposed by Navarro, Frenk & White (1995) will be considered in Section 5.

2.2 The correlation function

The previous subsection argued that the McClelland & Silk formalism can be used to compute to shape and amplitude of the correlation function in the non-linear regime. To do so requires knowledge of the density profiles of halos, as well as the number density of halos as a function of mass. It argued that the stable clustering hypothesis could be used to determine the density profiles of the halos. This section uses the Press & Schechter (1974) model to determine the mass function. Then, it combines the stable clustering density profile with the Press–Schechter mass function to compute the amplitude of the matter correlation function $\xi(r)$ in the non-linear regime.

In the stable clustering regime, we can use the McClelland & Silk formalism to express $\xi(r)$ as

$$\xi(r) = \frac{\mu \iint M^2 \lambda_\sigma(r) p(M, \sigma) dM d\sigma}{[\mu \iint M p(M, \sigma) dM d\sigma]^2}, \quad (5)$$

where μ is the total number density of halos, $p(M, \sigma) dM d\sigma$ is the probability that a halo has mass in the range dM about M and radius in the range $d\sigma$ about σ , and

$$\lambda_\sigma(r) = \int u_\sigma(\mathbf{s}) u_\sigma(\mathbf{s} + \mathbf{r}) d\mathbf{s}, \quad (6)$$

where u_σ describes the average density profile of a halo of radius σ (note the similarity to equation 2). Here, $\int_0^\sigma M u_\sigma(r) dr = M$, where M is the total mass of the halo. Thus, in this regime, $\xi(r)$ is determined solely by the distribution of masses, radii, shapes, and density profiles of halos. Below, we will combine the Press–Schechter model with the stable clustering hypothesis to specify these distributions.

In the Press–Schechter description of non-linear clustering, all matter is assumed to be contained within spherical virialized halos, and the distribution of halo masses is determined by the initial conditions. For a scale free initial spectrum $P(k) \propto k^n$ and $\Omega = 1$, the number density of halos with mass in the range dM about M is

$$n(M) dM = \frac{\bar{\rho}}{\sqrt{\pi}} \left(\frac{M}{M_*}\right)^{\frac{(n+3)}{6}} e^{-\left(\frac{M}{M_*}\right)^{\frac{(n+3)}{3}}} \left(\frac{n+3}{3}\right) \frac{dM}{M^2} \quad (7)$$

(Press & Schechter 1974; Lacey & Cole 1993). Here

$$M_* \propto a^{6/(n+3)} \quad (8)$$

is a characteristic mass which grows as the universe expands. This characteristic mass defines two scales. The first scale, which we will denote r_0 , is defined as follows. If the variance in the mass contained in randomly placed cells of radius r_0 is $1.68^2/2$, then the mean mass contained in these spheres is $M_* = (4\pi r_0^3/3) \bar{\rho}$, where $\bar{\rho} \propto a^{-3}$ is the background density

(e.g. Efstathiou et al. 1988). The second scale, denoted r_* , is the virial radius of an M_* halo, and is defined below.

The average density within each virialized halo is also known, so that the mass and radius of a virialized halo are related. For the halos described by equation (7) above, $M = (4\pi\sigma^3/3) \Delta_{\text{nl}} \bar{\rho}$, where $\Delta_{\text{nl}} = 178$, and $\bar{\rho}$ is the background density as before. Thus, in the Press–Schechter model, the distribution of halo masses, radii, and shapes are specified, whereas the density profiles of these halos are not. So, in the Press–Schechter approach, the correlation function in the non-linear regime is

$$\xi(r) = \frac{\int M^2 \lambda_M(r) n(M) dM}{[\int M n(M) dM]^2}, \quad (9)$$

where $n(M) dM$ is given by equation (7). Notice that equation (7) implies that the denominator in equation (9) is just $\bar{\rho}^2$. Moreover, notice that since $\lambda(r)$ (equation 6) is an expression like equation (2), equation (9) is exactly of the form discussed in the previous subsection. That is, it is a sum over all the different masses of terms like equation (2). This means that the shapes of the correlation function and the density profile are related to each other (equation 3).

To proceed, we need expressions for $\lambda_M(r)$, which in turn depend on the density profiles u_σ of the Press–Schechter halos. If we assume that these density profiles are power laws in distance from the halo center, then stable clustering requires that the density profile must be $u_\sigma \propto r^{-\epsilon}$ with ϵ given by equation (4). Thus, the Press–Schechter model specifies the number density of halos as a function of mass, as well as providing a relation between the mass and radius of each halo, and, in the non-linear regime, the stable clustering hypothesis specifies the density profiles of the Press–Schechter halos. So, by combining the Press–Schechter model with the stable clustering hypothesis, we are able to compute the shape and amplitude of $\xi(r)$.

If we use the stable clustering value, $\epsilon = 3(4+n)/(5+n)$, for the slope of the density profile of Press–Schechter halos, then we can compute $\lambda_M(r)$. For $-2 < n \leq 1$, we know that $\epsilon > 2$, so

$$\lambda_M(r) = \left(\frac{3-\epsilon}{4\pi\sigma^3}\right)^2 \frac{4\pi\sigma^{2\epsilon}}{r(\epsilon-2)} \times \int_{r/2}^\sigma [|s-r|^{2-\epsilon} - s^{2-\epsilon}] s^{1-\epsilon} ds, \quad (10)$$

for all $0 \leq r \leq 2\sigma$, and $\lambda_M(r) = 0$ otherwise. Similarly, when $n = -2$, so $\epsilon = 2$, then

$$\lambda_M(r) = \frac{1}{4\pi\sigma^2 r} \int_{r/2}^\sigma \ln \left| \frac{s}{r-s} \right| \frac{ds}{s} \quad \text{if } 0 \leq r \leq 2\sigma, \quad (11)$$

and $\lambda_M(r) = 0$ otherwise.

In the limit of vanishingly small separations,

$$\lambda_M(r) = \frac{1}{4\pi\sigma^3} \left(\frac{\sigma}{r}\right)^2, \quad \epsilon = 5/2, \quad n = 1, \quad (12)$$

$$\lambda_M(r) = \frac{1.22}{4\pi\sigma^3} \left(\frac{\sigma}{r}\right)^{1.8}, \quad \epsilon = 2.4, \quad n = 0, \quad (13)$$

$$\lambda_M(r) = \frac{1.58}{4\pi\sigma^3} \left(\frac{\sigma}{r}\right)^{1.5}, \quad \epsilon = 9/4, \quad n = -1, \quad (14)$$

$$\lambda_M(r) = \frac{\pi^2/4}{4\pi\sigma^3} \left(\frac{\sigma}{r}\right), \quad \epsilon = 2, \quad n = -2. \quad (15)$$

If we absorb all constants into one term, then we can write

$\lambda_M(r) = \lambda_n \sigma^{\gamma-3}/r^\gamma$, so that the correlation function is

$$\begin{aligned} \xi(r) &= \frac{\lambda_n}{r^\gamma \bar{\rho}^2} \left(\frac{4\pi \Delta_{\text{nl}} \bar{\rho}}{3} \right)^{\frac{2}{(5+n)}} \int M^{\frac{(3+n)}{(5+n)}} M n(M) dM \\ &= \frac{\lambda_n}{r^\gamma \bar{\rho}} \left(\frac{4\pi \Delta_{\text{nl}} \bar{\rho}}{3} \right)^{\frac{2}{(5+n)}} \frac{M_*^{\frac{(3+n)}{(5+n)}}}{\sqrt{\pi}} \Gamma\left(\frac{11+n}{10+2n}\right), \\ &= \left(\frac{r_*}{r}\right)^\gamma \left(\frac{\lambda_n}{\sqrt{\pi}} \frac{4\pi \Delta_{\text{nl}}}{3}\right) \Gamma\left(\frac{11+n}{10+2n}\right), \end{aligned} \quad (16)$$

where we have used the fact that $4\pi \Delta_{\text{nl}} \bar{\rho} \sigma^3/3 = M$. (Notice that this means that $r_*^3 = 3M_*/4\pi \Delta_{\text{nl}} \bar{\rho}$, so that r_* is quite a lot smaller than the scale r_0 on which the variance is $1.68^2/2$.) This, then, is the correlation function in the highly non-linear, stable clustering regime.

It is interesting to compare this result with that which we would have obtained had all halos had the same mass, say $M_{\text{halo}} = f^3 M_*$. In this case, equation (9) shows that the correlation function is just $\xi(r) = \lambda_n (4\pi \Delta_{\text{nl}}/3) (f r_*/r)^\gamma$, for $r < r_{\text{halo}}$, so that the amplitudes are comparable if $f^\gamma = \Gamma(11+n/10+2n)/\Gamma(1/2)$. Note that the amplitude increases as f increases, and is comparable to the Press–Schechter amplitude when M_{halo} is considerably less than M_* (0.42 and 0.125 times M_* , for $n = 1$ and $n = -2$, respectively).

2.3 Comparison with simulations

To illustrate the accuracy of the amplitude predicted by equation (16), we can compare it directly with that measured in the N -body simulations of clustering from scale free initial conditions. A simple and reliable way to make the comparison is to use recently proposed fitting formulae for the non-linear ξ which have been calibrated using high resolution N -body simulations. These are based on the ansatz of Hamilton et al. (1991) which provides a universal relation between the linear and non-linear correlation function (also see Gott & Rees 1975). This ansatz has recently been extended and refined (Nityananda & Padmanabhan 1994; Peacock & Dodds 1994; Padmanabhan et al. 1995; Padmanabhan 1995; Jain, Mo & White 1995 – JMW). We shall use the fitting formulae proposed by JMW which take into account a simple dependence on the shape of the initial spectrum that is exhibited by the N -body data.

In the asymptotic non-linear regime the formulae are consistent with stable clustering and take the form (see equations (5a) and (6a) of JMW),

$$\bar{\xi}_{\text{NL}}(a, x) \approx \frac{50}{3} \left(\frac{3+n}{3}\right)^{-0.4} \bar{\xi}_{\text{L}}(a, l)^{3/2} \quad (17)$$

where,

$$l^3 \approx x^3 \bar{\xi}_{\text{NL}}(a, x); \quad \bar{\xi}(x) = \frac{3}{x^3} \int_0^x dy y^2 \xi(y). \quad (18)$$

Here, $\bar{\xi}(a, x)$ is the volume integral of the correlation function over a sphere of comoving radius $x = r/a$ (the subscripts refer to the non-linear and the linear regimes, respectively). Since $\bar{\xi}_{\text{L}}(a, l) \propto l^{-(n+3)}$, it is easy to see that the correlation function in equation (16) has the same scaling as equation (17).

The predicted amplitudes of the non-linear correlation function (equations 16 and 17) can be compared after

Table 1. Comparison of the amplitude of the non-linear ξ

n	N_{sc}	N_{jmw}	Fractional “Error”
0	3.5	3.1	13 %
-1	5.1	5.0	2 %
-2	17.4	13.7	27 %

some straightforward simplifications. For the initial spectrum $P(k) = A k^n$, the expression in equation (16) can be written as

$$\xi_{\text{sc}}(a, r) = A N_{\text{sc}}(n) a^{\frac{6}{(5+n)}} r^{-\gamma}, \quad (19)$$

where N_{sc} contains all the normalization factors. Also, equation (17) simplifies to,

$$\xi_{\text{jmw}}(a, r) = A N_{\text{jmw}}(n) a^{\frac{6}{(5+n)}} r^{-\gamma}. \quad (20)$$

So, the task of comparing the amplitude of ξ to the N -body calibrated formula simplifies to a comparison of the normalization constants $N_{\text{sc}}(n)$ and $N_{\text{jmw}}(n)$. The results for the cases $n = 0, -1$, and -2 are shown in Table 1. Note that, for the $n = -2$ case, the agreement between our prediction and the N -body data is better than indicated in the table because, as noted by JMW, their formula underestimates the non-linear amplitude of ξ for this spectrum.

We can also compare the amplitude predicted by equation (16) directly with that measured in the N body simulations of Efstathiou et al. (1988). Their Fig. 4 shows $\log_{10} \Xi$ where $\Xi = (x/L)^\gamma \xi(x/L)$ for $-2 \leq n \leq 1$. At late times, so that discreteness effects are less important, the amplitudes of their correlation functions scale as $a^{6/(5+n)}$. This scaling is consistent with that of equation (16). At the final output time in their simulations $\log_{10} \Xi = -1.6, -1.4$, and -0.9 for $n = 1, 0$, and -1 , respectively. If we set $\Delta_{\text{nl}} = 178$ and use the fact that, in their simulations, $\bar{\rho} = 32^3/(aL)^3$ and $M_* = C_n a^{6/(3+n)}$, where $C_n = 0.8, 0.71$, and 0.53 (their eq. 15), then equation (16) predicts that $\log_{10} \Xi = -1.6, -1.3$, and -0.8 , respectively. Thus, our predicted amplitudes (equation 16) and those measured in the JMW and the Efstathiou et al. simulations agree to within about 20%. Some of this discrepancy is probably due to the fact that the Press–Schechter mass functions provide good, but not perfect, fits to the halo size distribution in the simulations. We conclude that equation (16) provides a good description of the shape and amplitude of the correlation function in the highly non-linear regime.

3 RELATION TO SECONDARY INFALL MODELS OF SPHERICAL COLLAPSE

The calculation of the previous section assumed that Press–Schechter halos are spherical, with density profiles having slope $\epsilon = 3(4+n)/(5+n)$. That is, the previous section provided a relation between the initial fluctuation spectrum and the density profiles of non-linear, spherical, virialized halos (equation 4). It also showed that the correlation function that corresponds to this choice for the relation between ϵ and n is in good agreement with that measured in N -body simulations. However, this relation between ϵ and n can be tested more directly.

Recently, Crone et al. (1994) measured density profiles of virialized halos in their initially scale free simulations. Although they did not compare their measurements with the relation of equation (4), their simulations show that it is remarkably accurate. Therefore, it is interesting to see if this relation can be derived directly from models of spherical collapse, rather than from the combination of the Press–Schechter model with the stable clustering hypothesis used in the previous section.

It is well known that if the initial density profile of a halo is a power law in radius (a ‘cone-hat’, rather than a ‘tophat’), then the density profile of the collapsed halo is also a power law. If the initial density profile is $\rho \propto r^{-\alpha}$, then the collapsed halo has slope

$$\epsilon = \frac{3\alpha}{1 + \alpha} \quad \text{if } \alpha < 2, \quad (21)$$

and $\epsilon = -2$ if $\alpha < 2$ (Fillmore & Goldreich 1984). If one allows for non-radial orbits, then the restriction on α can be relaxed (White & Zaritsky 1992). This solution describes the shape of a single collapsed halo. If, instead, we start with a distribution of halos identified in an initially Gaussian random field, then the question is: What is the initial density profile of a typical halo? Once we know the answer, we can set this value equal to α in equation (21), and so calculate the typical density profile of collapsed halos.

Hoffman & Shaham (1985) argue that the initial progenitor halos may be related to peaks in the initial density field. The density profiles of very high peaks have the same r dependence as the correlation function of the underlying field (Section VII in Bardeen et al. 1986). Since the correlation function of the initial (scale free) field is $\propto r^{-(3+n)}$, Hoffman & Shaham set $\alpha = 3 + n$ in equation (21) to obtain $\epsilon = 3(3 + n)/(4 + n)$. This dependence on n is different from that in equation (4). However, it is not clear that the Hoffman–Shaham value for α is the relevant one. This is because, as the peak height decreases, the peak profile becomes steeper than the correlation function (Fig. 8 in Bardeen et al. 1986). As the universe expands, peaks of smaller and smaller height are able to collapse, so it is important to account for this difference between the average peak profiles and the shape of the initial correlation function.

The mean peak profile, averaged over all curvatures and orientations, depends, to a good approximation, on a sum that involves the initial correlation function and its second derivative (equation 7.10 in Bardeen et al. 1986). For initially scale free fields, the correlation function is $\propto r^{-(3+n)}$ so that its second derivative is $\propto r^{-(5+n)}$. Thus, setting $\alpha = 4 + n$ should give some indication of the shapes of collapsed peaks, when the initial peaks are not arbitrarily high. This value for α in equation (21) gives $\epsilon = 3(4 + n)/(5 + n)$ for $-2 \leq n \leq 1$. While it is interesting that this relation between the non-linear density profile and the initial fluctuation field is the same as that obtained in the previous section using the stable clustering hypothesis, one would prefer a more rigorous derivation.

4 THE ONSET OF STABLE CLUSTERING

Section 2 used the fact that the shape of the correlation function in the non-linear, stable clustering regime is related to

the average density profile and mass distribution of virialized halos. It did not address the question of the scale on which stable clustering becomes a good approximation. The usual assumption is that stable clustering is accurate when the density contrast is on the order of that required for virialization: $\Delta_{n1} \sim 200$. On the other hand, N -body simulations show that the onset of stable clustering occurs at higher density contrasts as n , the slope of the power spectrum of initial fluctuations, increases (Jain 1995). This section uses the Press–Schechter description of clustering to show why this might be expected.

Essentially, this section is motivated by the fact that not all Press–Schechter halos at the epoch t_1 evolve to become cores of halos by the epoch $t_2 > t_1$. For example, one might reasonably expect that for a halo of mass M_2 at the epoch t_2 , the most massive subhalo $M_1 < M_2$ at the epoch t_1 becomes the core. If the density profile of M_2 at t_2 has the slope obtained in the previous section, then some or all of the other subhalos that make up the mass ($M_2 - M_1$) may have been destroyed as they merged to form the final halo. This disruption of subhalos as they merge to form larger halos has been seen in N -body simulations (e.g. Fig. 2 in Efstathiou et al. 1988). These disrupted subhalos will not have evolved in accordance with the stable clustering hypothesis. So, only the (most massive?) progenitor subhalo in the core is likely to have evolved consistently with both Press–Schechter and stable clustering. This has the following consequence.

It is usual to assume that stable clustering should be a good approximation on scales that are comparable to that of a typical Press–Schechter halo. This corresponds to scales on which the density is on the order of ~ 200 times the background density. However, the discussion above suggests that the objects that are not in the core of a Press–Schechter halo may not satisfy the stable clustering hypothesis. Therefore, the relevant density contrast for the onset of stable clustering is that associated with the core of the halo, rather than of the halo itself. Suppose we assume that the core size is the scale associated with the typical size of the most massive progenitor of a given halo. Since the core is smaller (and more dense) than the halo itself, one might reasonably expect that stable clustering will only be a good approximation once the density contrast is somewhat larger than the canonical value of ~ 200 or so.

To be more quantitative, consider a halo with mass M_0 at time t_0 , and assume that a stable core was formed in its center when one of its progenitor subhalos had a mass of $M_0/2$. To estimate the density of this half-mass core, we must estimate the scale associated with this core, which, by the stable clustering assumption, is the same physical scale it had at the epoch at which it virialized. So, we must estimate the earliest epoch at which half the mass of the halo was first assembled into a virialized subhalo of mass $M_0/2$. There are two ways to do this. The first is to use the fact that

$$P(M_1 > M_0/2, t_1 | M_0, t_0) = \text{erfc} \left(\frac{\bar{\omega}}{\sqrt{2}} \right), \quad (22)$$

where $P(M_1 > M_0/2, t_1 | M_0, t_0)$ denotes the probability that a mass element of M_0 was previously in an object of mass $M_1 > M_0/2$ at the epoch t_1 , and where

$$\bar{\omega} = \frac{\delta(t_1) - \delta(t_0)}{\sqrt{(\sigma_0^2(M_0/2) - \sigma_0^2(M_0))}}, \quad (23)$$

where $\delta(t)$ describes the (linear theory) overdensity required for collapse at time t (it decreases as the inverse of the expansion factor), and $\sigma_0^2(M)$ is the variance of the linear density field when smoothed with a filter containing mass M (see Lacey & Cole 1993 for details). Then, setting $P = 1/2$ gives an estimate of $\delta(t_1) \equiv \delta(t_f)$ at the time t_f of formation. Since $\text{erfc}(x) = 1 - \text{erf}(x) = 1/2$ when $x \approx 0.4769$, this means that $\bar{\omega}_f = 0.4769 \sqrt{2} = 0.67$. This way of estimating the halo formation time has been used by Navarro, Frenk & White (1995).

However, as Lacey & Cole (1993) note (and their Fig. 7 shows), this method provides a biased estimate of the formation time. They show that a more precise estimate of the formation time is obtained by noting that, with this (half-mass assembled) definition of formation, different halos, each of mass M_0 , may have formed at different times. So, one should compute the distribution of formation epochs, and then compute the mean, or the most probable value, of this distribution. For initially scale free fields, the most probable value of the formation epoch, t_f , is given by

$$1 + z_f = \left(\frac{t_0}{t_f}\right)^{2/3} = 1 + W_f \sqrt{2^\beta - 1} \left(\frac{M_*}{M_0}\right)^{\beta/2}, \quad (24)$$

where $\beta = (n + 3)/3$, and $W_f \approx 0.75$ (see Fig. 7 and equation 2.32 in Lacey & Cole 1993). This estimate differs slightly from the estimate of the previous paragraph, for which $W_f \approx 0.67$.

Equation (24) shows that the formation epoch is mass dependent. Fig. 1 shows this distribution of formation epochs for $-2 \leq n \leq 1$, with $W_f = 0.7$ (the curves for $W_f = 0.67$ and 0.75 are very similar to the one shown). Two features are obvious. Halos that are less massive than about $10M_*$ or so form earlier (at higher z_f) for large n than for small n . On the other hand, halos that are more massive than this scale with n in the opposite sense. It is easy to see that both these features are a consequence of two facts. Namely, the distribution of Press–Schechter halo sizes becomes broader as n decreases; when $n = 1$ most halos have the characteristic mass M_* , but when $n = -2$, many halos have significantly different masses. So, if $n = 1$ initially, then halos that are significantly more massive than the characteristic mass at, say, the present time must have formed very recently (i.e., at low redshift), since they are extremely unlikely to have existed at early times when the characteristic mass was lower. In contrast, if $n < -1$ initially, then some of these more massive halos may easily have been formed at earlier times (higher redshifts). Furthermore, the growth rate of the characteristic mass is more rapid for small values of n (equation 8). Therefore, the asymptotic power law behaviour shown in the figure (for small M/M_* as a function of $1 + z_f$) is a direct consequence of equation (8).

So, the way in which the epoch of formation of cores scales with n depends on the ratio M/M_* . However, most of the mass is in halos with masses $M \leq M_*$ (the actual fraction is $\text{erf}(1) = 0.84$). This means that, for large n , most of the stable cores will virialize at earlier times than for lower n . By the Press–Schechter hypothesis, progenitor cores will have had an average density of ~ 200 times the background density when they virialized (at z_f). This sets the scale of the halo. Stable clustering implies that, in physical coordinates, the size of the core does not change, so that, by t_0 , its comoving density will have increased by the cube of the expansion

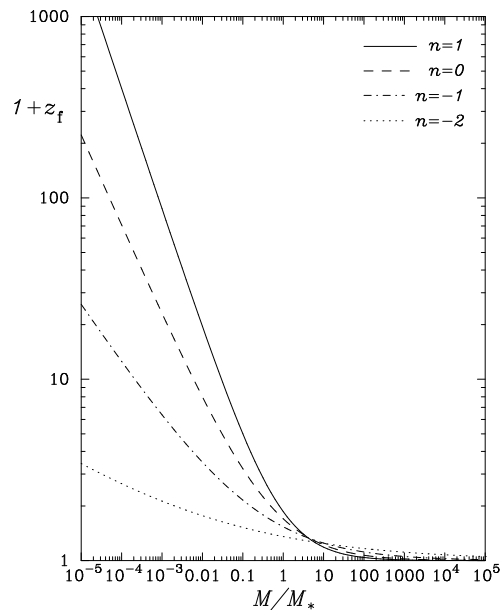


Figure 1. The epoch of formation z_f for halos with mass M/M_* , for various choices of n .

factor since the time t_f when it virialized. So, on average, the average density of stable cores of Press–Schechter halos increases as n increases. Since stable clustering is only a good approximation in these cores, the density contrast on which stable clustering becomes a good approximation increases as n increases.

We can estimate the amplitude of the correlation function at which stable clustering becomes accurate as follows. Assume that, when averaged over all halos, the onset of stable clustering occurs at the half-mass radius of a halo with mass $M = f^3 M_*$, where f was given at the end of section 2.2. Recall that this definition of f was chosen so that, if all halos had this same mass, rather than the Press–Schechter distribution of masses, then the $r \rightarrow 0$ amplitude of the correlation function would be unchanged. The ratio of this half-mass radius to the virial radius of such a halo is $0.5^{1/(3-\epsilon)}$. On this scale, the correlation function is $\xi \gtrsim \lambda_n (4\pi\Delta_{\text{nl}}/3) 2^{7/(3-\epsilon)}$ which implies $\xi \gtrsim 300$ for $n = -2$ and $\xi \gtrsim 600$ for $n = 0$. This increase of the requisite amplitude of ξ as n increases is in qualitative agreement with recent measurements of the onset of stable clustering in N -body simulations for which $\xi \gtrsim 200$ for $n = -2$ and $\xi \gtrsim 1000$ for $n = 0$ (Jain 1995).

5 DISCUSSION

We have shown that requiring consistency between the stable clustering hypothesis and the Press–Schechter approach suggests that the density profiles of Press–Schechter halos should be power laws with slope $\epsilon = 3(4+n)/(5+n)$, where n is the slope of the initial fluctuation spectrum (equation 4). This value differs from that expected from secondary infall studies of the collapse of peaks associated with initially Gaussian fields (Hoffman & Shaham 1985). The reasons for this difference were discussed in Section 3.

The Press–Schechter model, with the stable clustering

density profile, was used to compute the amplitude of the correlation function in the highly non-linear regime (Section 2). This amplitude was shown to be in good quantitative agreement with that measured in N -body simulations. Moreover, the amplitude was shown to be a function of the slope n of the initial power spectrum. The n -dependence resembles that which was obtained recently by Jain et al. (1995) and Padmanabhan et al. (1995).

Our calculation of ξ (equation 5) rests on the assumption that, in this (small separation) regime, the correlation function is determined primarily by the density profiles of virialized halos. That is, the crucial assumption is that, for these small separations, most pairs are most likely to be drawn from the same halo, so that correlations between different halos have a negligible effect on the shape of ξ . While this assumption makes intuitive sense, we have yet to show that it is accurate. We can do this as follows.

Equation (9) shows that the correlation function can be written as a sum over halos of different masses. To demonstrate that our approach is at least self-consistent, we must show that the correlation function is, indeed, determined primarily by halos having diameters that are larger than the separation scale r . So, consider the limit $r \rightarrow 0$ of vanishingly small separations. Then the amplitude of the correlation function is given by equation (16). Of course, in this limit, all halos are larger than the separation scale. However, as a crude approximation that should also give some indication of the result on slightly larger scales, we will compute the fractional contribution to ξ from ‘small’ halos, which we will define to be all those with $M/M_* \leq 0.2$. Equation (16) shows that this contribution is simply an incomplete Gamma function. Thus, the small mass contribution is

$$\gamma\left[\frac{11+n}{10+2n}, 0.2^{n+3/3}\right] / \Gamma\left[\frac{11+n}{10+2n}\right],$$

which is 11, 15, 20, and 24 per cent for $n = 1, 0, -1$ and -2 respectively. For non-zero values of r , the corresponding integrals can be done numerically. They also show that ξ is determined primarily by pairs within larger halos, so that our neglect of halo-halo correlations is justified.

The other crucial ingredient in our calculation is knowledge of the density profiles of virialized halos. We assumed that these profiles were power laws, and determined the slopes of the power laws by requiring that they yield a correlation function with the shape required by stable clustering. However, recent work suggests that, while the profile shape may be described by an average power law slope that is consistent with equation (4), the density profiles of halos that form in N -body simulations of gravitational clustering from scale free initial conditions are not simple power laws (Navarro, Frenk & White 1995; Cole & Lacey 1995; Tormen 1995). Rather, the density profiles seem to be well fitted by a function of the form $\rho \propto 1/[r(r+b)^2]$, where the core radius b depends both on the mass M and the shape of the initial power spectrum.

We expect our formalism to work for these non-power-law profiles also because, except for the inner regions $r \sim 0.1 r_{\text{vir}}$, where r_{vir} is the virial radius, they are reasonably well described by the power-law profiles we have been considering. To illustrate this, Fig. 2 shows the non-power law profile $\rho(s) \propto 1/[s(s+a)^2]$, where $s = r/r_{\text{vir}}$ and the core radius is given by $a = b/r_{\text{vir}}$. The plot shows this profile for

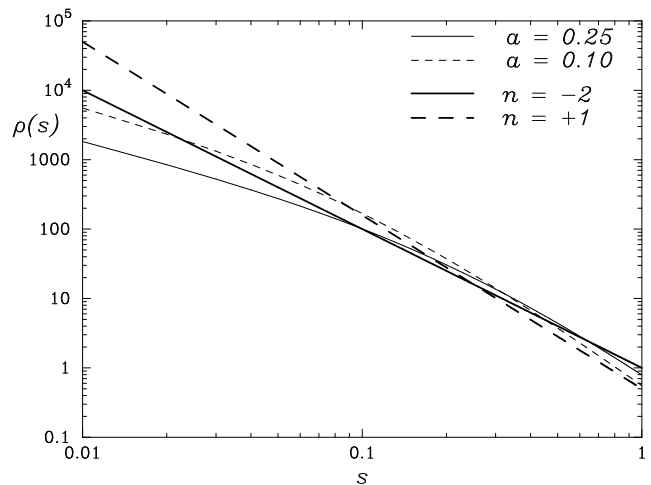


Figure 2. The density profile $\rho(s) \propto 1/[s(s+a)^2]$, where $s = r/r_{\text{vir}}$, $a = b/r_{\text{vir}}$, and b is the core radius, for a range of values of a . When $s \gtrsim 0.1$, the power law profile that corresponds to $n = -2$ (solid bold curve) describes the $a = 0.25$ profile quite well. The dashed bold curve shows the power law corresponding to the $n = 1$ case; when $s \gtrsim 0.1$ it fits the $a = 0.1$ profile reasonably well.

a range of values of the scaled core radius a . These values were chosen because N -body simulations show that $a \sim 0.25$ describes the $n = -2$ simulations quite well, whereas a is smaller (~ 0.15) when $n = 0$ (Cole & Lacey 1995). For comparison, the thicker curves show the corresponding stable clustering power law profiles for the two extreme cases studied here, $n = -2$ and $n = 1$. Notice that, in the outer regions where $s \gtrsim 0.1$, the $n = -2$ (solid bold) curve describes the $a = 0.25$ profile quite well, whereas the $n = 1$ (dashed bold) curve fits the $a = 0.1$ profile.

Now, the correlation function in the non-linear regime is essentially an integral over the density profile (to give λ_M), followed by an integral over the mass function. For the choices of n and a shown in Fig. 1, the corresponding $\lambda_M(r)$ curves for the power law and the non-power law cases are similar, on scales larger than about $0.1 r_{\text{vir}}$. This is hardly surprising, since Fig. 2 shows that the Navarro et al. and power law density profiles $\rho(s)$ are similar in the outer regions where $s \gtrsim 0.1$ (which contain most of the mass of a halo), and λ_M is simply the density profile convolved with itself.

Since, in our formalism, ξ is simply the sum of many λ_M curves, this suggests that ξ for these non-power law profiles should be similar to that for the power law profiles considered in Section 2, at least for separations that are on the order of about $0.1 r_*$ and larger. We have verified that this is indeed the case: for scales on which $\xi(r) \lesssim 1000$, the predicted amplitude of ξ changes by less than about 10% for $-2 < n < 1$, if we use the Navarro et al. profile (with the values of a shown in Fig. 1) instead of power law profiles.

On scales smaller than $\sim 0.1 r_*$, it is necessary to take into account the dependence of the core radius on the mass of the halo. Simulations show that, typically, a decreases as M decreases. Navarro et al. (1995) argue that the qualitative form of this relation can be understood in terms of the formation times of Press-Schechter halos. Including this trend improves the agreement of our predicted ξ with the result

from the Navarro et al profile. The asymptotic behavior of $\xi(r)$ as $r \rightarrow 0$ however, is more subtle, as it is very sensitive to the $M \rightarrow 0$ behavior of the core radius a and the Press-Schechter $n(M)$. Here we simply note that by requiring that $\xi(r)$ have the stable clustering shape, we can obtain an independent constraint on the relation between a , M , and n for these non-power law profiles.

Since all of the results of this paper concern the stable clustering regime, Section 4 discussed the scale on which stable clustering should become a good approximation. It used the Lacey & Cole (1993) analysis of the merger histories of Press-Schechter halos to show that the onset of stable clustering occurs at higher density contrasts as the slope of the initial fluctuation power spectrum n increases. This is in qualitative agreement with N -body simulations (Jain 1995).

Our derivation of the amplitude of the correlation function in the stable clustering regime, using the Press-Schechter mass multiplicity function, can be extended to cosmological models in which $\Omega \leq 1$. This is because the effect of Ω on the density profiles of halos has been calculated (e.g. Hoffman & Shaham 1985; Hoffman 1988; White & Zaritsky 1992), as has the effect on the evolution of the Press-Schechter mass function (Lacey & Cole 1993). Furthermore, recall that both the density profiles and the Press-Schechter multiplicity function depend strongly on the shape of the initial power spectrum. Thus, our calculation of ξ shows explicitly how the non-linear correlation function depends on the shape and amplitude of the linear power spectrum. Therefore, if our approach is correct, then by requiring consistency between the shape of the mass multiplicity function and the shape of the non-linear correlation function, one can estimate the shape and amplitude of the initial perturbation spectrum.

ACKNOWLEDGMENTS

We thank Gerard Lemson for sending us copies of his insightful Ph.D. thesis, and Simon White and Saleem Zaroubi for many stimulating discussions and helpful suggestions.

REFERENCES

- Bardeen J. M., Bond J. R., Kaiser N., Szalay A. S., 1986, ApJ, 304, 15
 Cole S., Lacey C., 1995, astro-ph/9510147
 Davis M., Peebles P.J.E., 1977, ApJS, 34, 425
 Efstathiou G., Frenk C., White S. D. M., Davis M., 1988, MNRAS, 235, 715
 Fillmore J., Goldreich P., 1984, ApJ, 281, 1
 Gott III J. R., Rees M., 1975, A&A, 45, 365
 Hamilton A. J. S., Kumar P., Lu E., Matthews A., 1991, ApJ, 374, L1
 Hoffman Y., 1988, ApJ, 328, 489
 Hoffman Y., Shaham J., 1985, ApJ, 297, 16
 Jain B., 1995, astro-ph/9509033
 Jain B., Mo H. J., White S. D. M., 1995, MNRAS, 276, L25
 Lacey C., Cole S., 1993, MNRAS, 262, 627
 Lemson G., 1995, PhD thesis, University of Groningen
 McClelland J., Silk J., 1977, ApJ, 217, 331
 Navarro J., Frenk C., White S. D. M., 1995, astro-ph/9508025
 Nityananda R., Padmanabhan T., 1994, MNRAS, 271, 976

- Padmanabhan T., 1993, Structure Formation in the Universe. Cambridge Univ. Press, Cambridge
 Padmanabhan T., Cen R., Ostriker J.P., Summers F.J. 1995, astro-ph/9506051
 Padmanabhan T., 1995, astro-ph/9510037
 Peebles P. J. E., 1965, ApJ, 142, 1317
 Peebles P. J. E., 1974a, ApJ, 189, L51
 Peebles P. J. E., 1974b, A&A, 32, 197
 Peebles P. J. E., 1980, The Large Scale Structure of the Universe. Princeton Univ. Press, Princeton
 Press W., Schechter P., 1974, ApJ, 187, 425
 Tormen G., 1995, astro-ph/9512130
 White S. D. M., Zaritsky D., 1992, ApJ, 394, 1